# The Impact Of Changing Magnetization Reactance Value On The Performance Of Three-Phase Induction Motor

# Asuquo Eke, O. I. Okoro, A. J. Onah.

Department Of Electrical/Electronic Engineering, University Of Cross River State, Calabar, Nigeria Department Of Electrical/Electronic Engineering, Michael Okpara University Of Agriculture, Umudike. Abia State. Nigeria.

#### Abstract

The motor design for the three-phase induction motor under study was completed in this research using ANSYS Motorcad. The impact of variations in magnetization reactance (Rm) values on motor performance is often examined in these investigations. Efficiency, torque, current, and power factor were all taken into account in this work. Analysis and findings were achieved for magnetization reactance values between 0.5 and 2.5. Table 3.0 provides a summary of the findings, while Figures 1, 2, and 3 illustrate the effects. The flux distribution for the motor under study in the Motorcad environment is displayed in Figure 4.0. The findings show that at Rm=0.5, the torque is 3Nm, the efficiency is 61.5%, the current is 3.3A, and the power factor is 0.75%. Efficiency is 75%, torque drops to 2.55 Nm, current is 1.25A, and power factor is 0.8% at Rm=1.0. Efficiency is 80%, torque is 1.82 Nm, current is 1.1 A, and power factor is 0.7% when Rm=1.5. 85% motor efficiency, 0.3 Nm torque, 1.0 A current, and a stable power factor are achieved with Rm=2.5. Since Rm values are components of magnetization current, they have an impact on no-load losses.

**Keyword:** Magnetization Reactance, Three-Phase Induction Motor, Motor Performance, Impedance Variation, Electrical Machine Analysis

Date of Submission: 01-11-2025 Date of Acceptance: 10-11-2025

#### I. Introduction

The magnetizing resistance (Rm) is a critical parameter in induction motor design and operation, playing a significant role in determining the motor's performance characteristics. Rm represents the opposition to the magnetizing current in the motor, which is essential for creating the magnetic field that enables the motor to produce torque Okoro (2003), Eke, et al (2024). The magnetization reactance (Xm) is an important factor in the performance of a three-phase induction motor. It is a component of the motor's equivalent circuit that indicates the magnetizing current necessary to create a magnetic field in the stator and rotor of the motor. When the magnetization reactance changes, various aspects of the motor's performance are affected, including Perduková, et al (2020). The magnetization reactance controls how much magnetizing current is needed to generate a magnetic field in the motor. A greater Xm number indicates a larger magnetizing current, while a lower Xm value indicates a lower magnetizing current. The magnetizing current accounts for a sizable amount of the motor's noload current draw. Liang et al (2017), Park, et al. (2024). The no-load current will grow as Xm increases. A drop in Xm, on the other hand, will result in a decrease in no-load current. The magnetizing current is roughly 90 degrees ahead of the voltage, resulting in a trailing power factor under no-load conditions. Changes in Xm can affect the magnitude of the reactive power component and, as a result, the power factor. The magnetization reactance affects the magnetic flux in the air gap of the motor. A larger Xm value causes more magnetic flux, which affects the motor's performance, torque, and efficiency. A significant magnetizing current is required to establish the magnetic field during motor starting. Changes in Xm can have an impact on the beginning current and torque. Park, et al (2024). In an induction motor, the magnetization reactance (Xm) is a rotor's equivalent circuit component. It denotes the reactance associated with the magnetizing current necessary to create a magnetic field in the rotor of the motor. The magnetization reactance influences no-load losses, which include iron losses in the rotor caused by the magnetizing current. When Xm grows, so do the iron losses, resulting in a decline in the motor's efficiency at full load. Reduced Xm, on the other hand, can boost efficiency by lowering these losses. Park, et al (2023). At low loads, core losses, including those produced by the magnetizing current, account for a larger proportion of total losses. The core losses grow as Xm increases, lowering the motor's efficiency at light loads. Under light load conditions, a lower Xm can aid in improving efficiency Aoyama, et al (2021). The magnetizing current travels through the rotor windings, causing copper losses. Higher magnetizing current and copper losses come from increasing Xm. This additional copper loss affects the efficiency of the motor. Reduced Xm, on the other hand, can reduce copper losses and improve overall efficiency. Banchhor, et al. (2018). The magnetizing current is required during motor startup to generate the initial magnetic flux in the rotor. A greater

DOI: 10.9790/0853-2006010108 www.iosrjournals.org 1 | Page

Xm number raises the starting current, resulting in a poorer starting efficiency. Reducing Xm can help increase the motor's starting efficiency. Ejiofor, et al (2019), Dey et al (2008), Sengamalai, et al (2022). Because of the higher reactive component of the magnetizing current, a bigger Xm results in a lower power factor; a lower Xm value results in a better power factor, which raises overall efficiency reactance affects the motor's power factor. [Park, et al. (2024).

#### Mathematical Modelling And Equivalent Circuit Of Three-Phase Induction Motor

The dynamic model equations of the induction motor according to Okoro (2003) can be obtained from the dq0 equivalent circuit of the induction motor shown in Figure 1.1, figure 1.2.

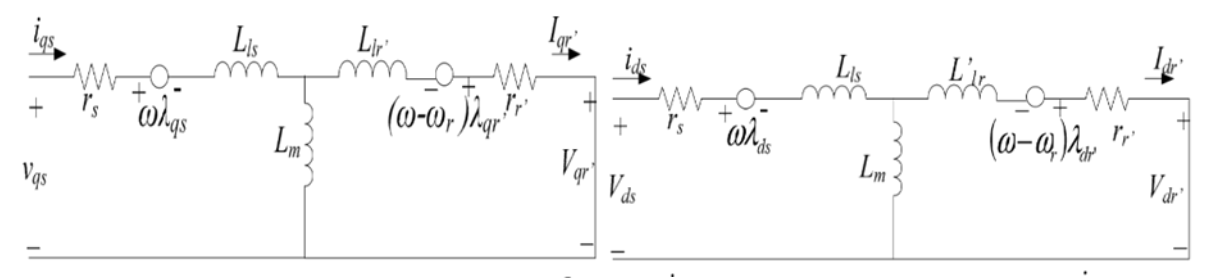


Fig. 1. D-axis equivalent circuit of an induction motor Okoro (2003)

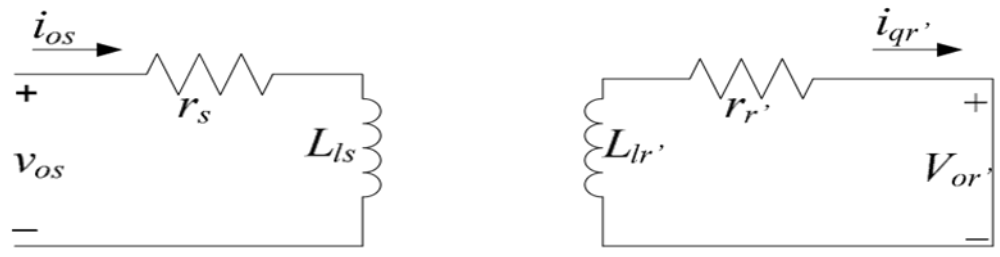


Fig. 1.2. Q-axis equivalent circuit of an induction motor Okoro (2003)

Under balanced conditions the three-phase stator voltage of an induction motor can be expressed as

$$Va = \sqrt{2} \text{ Vrms sin}(\omega t) \tag{1}$$

Vb = 
$$\sqrt{2}$$
 Vrms sin  $\left(\omega t - \frac{2\pi}{3}\right)$  (2)

$$Vc = \sqrt{2} \text{ Vrms sin} \left( \omega t + \frac{2\pi}{3} \right)$$
 (3)

These three-phase voltages are transformed into two-phase synchronously rotating reference frames of dq0 axis.

$$\begin{bmatrix} V_{\alpha} \\ V_{\beta} \end{bmatrix} = \frac{2}{3} \begin{bmatrix} 1 & \frac{1}{2} & -\frac{1}{2} \\ 0 & \frac{\sqrt{3}}{2} & -\frac{\sqrt{3}}{2} \end{bmatrix} \begin{bmatrix} V_{\alpha} \\ V_{b} \\ V_{c} \end{bmatrix}$$
 (4)

Then, the dq axis voltages
$$\begin{bmatrix} V_d \\ V_q \end{bmatrix} = \begin{bmatrix} \cos \theta & \sin \theta \\ -\sin \theta & \cos \theta \end{bmatrix} \begin{bmatrix} V_{\alpha} \\ V_{\beta} \end{bmatrix}$$
(5)

The instantaneous value of the stator and rotor currents of a three-phase induction motor is calculated by using the following matrix equations (6) and (7); Montaser et al (2025

$$\begin{bmatrix} \mathbf{i}_{\alpha} \\ \mathbf{i}_{\beta} \end{bmatrix} = \begin{bmatrix} \cos \theta & -\sin \theta \\ \sin \theta & \cos \theta \end{bmatrix} \begin{bmatrix} \mathbf{i}_{d} \\ \mathbf{i}_{q} \end{bmatrix} \tag{6}$$

$$\begin{bmatrix} i_a \\ i_b \\ i_c \end{bmatrix} = \begin{bmatrix} 1 & 0 \\ \frac{1}{2} & -\frac{\sqrt{3}}{2} \\ -\frac{1}{2} & -\frac{\sqrt{3}}{2} \end{bmatrix} \begin{bmatrix} i_a \\ i_\beta \end{bmatrix}$$
 (7)

The stator and rotor voltage equation of the direct and quadrature (d-q) axis of an induction motor are given in equations (8), (9), (10), and (11). Eke, et al (2024)

$$V_{qs} = R_s i_{qs} + \frac{d}{dt} \lambda_{qs} + \omega_e \lambda_{qr}$$
 (8)

$$V_{qs} = R_s i_{qs} + \frac{d}{dt} \lambda_{qs} + \omega_e \lambda_{qr}$$
(8)  

$$V_{ds} = R_s i_{ds} + \frac{d}{dt} \lambda_{qs} - \omega_e \lambda_{ds}$$
(9)  

$$V_{qr} = R_r i_{qr} + \frac{d}{dt} \lambda_{qr} + (\omega_e - \omega_r) \lambda_{qr}$$
(10)

$$V_{qr} = R_r i_{qr} + \frac{d}{dt} \lambda_{qr} + \left( \omega_e - \omega_r \right) \lambda_{qr}$$
 (10)

$$V_{dr} = R_r i_{dr} + \frac{d}{dt} \lambda_{dr} - \left(\omega_e - \omega_r\right) \lambda_{dr}$$
 (11)

Where,  $\lambda_{ar}$ ,  $\lambda_{as}$ ,  $\lambda_{dr}$ , and  $\lambda_{ds}$  are the stator and rotor flux linkage of the d and q axis, these equations show the synchronously rotating reference frame for the two-phase d-q-axis of the induction motor. Okoro (2003) For squirrel cage induction motor, the rotor voltages  $V_{qr}$ ,  $V_{dr}$  are set to zero, since the rotor cage bars are shorted. Therefore, the flux linkage equation can be expressed as equations (12), (13), (14), (15), (16), (17), and (18). Ali et al (2024), Montaser et al (2025

$$\frac{d\lambda_{qs}}{dt} = \omega_b \left[ V_{qs} - \frac{\omega_e}{\omega_b} \lambda_{ds} + \frac{R_s}{X_{ls}} (\lambda_{mq} - \lambda_{qs}) \right]$$
(12)

$$\frac{d\lambda_{ds}}{dt} = \omega_{b} \left[ V_{ds} + \frac{\omega_{e}}{\omega_{h}} \lambda_{qs} + \frac{R_{s}}{X_{ls}} (\lambda_{md} - \lambda_{qs}) \right]$$
(13)

$$\frac{d\lambda_{qr}}{dt} = \omega_{b} \left[ V_{qs} - \left( \frac{\omega_{e-\omega_{r}}}{\omega_{b}} \right) \lambda_{qr} + \frac{R_{r}}{X_{lr}} (\lambda_{mq} - \lambda_{qr}) \right]$$

$$\frac{d\lambda_{qr}}{dt} = \omega_{b} \left[ V_{qs} + \left( \frac{\omega_{e-\omega_{r}}}{\omega_{b}} \right) \lambda_{qr} + \frac{R_{r}}{X_{lr}} (\lambda_{mq} - \lambda_{qr}) \right]$$

Where:

$$\lambda_{mq} = X_{ml} \left[ \frac{\lambda_{qs}}{X_{ls}} + \frac{\lambda_{qr}}{X_{ls}} \right] \tag{16}$$

$$\lambda_{\mathrm md} = \mathrm{X}_{ml} \left[ \frac{\lambda_{\mathrm qs}}{\mathrm{X}_{\mathrm lc}} + \frac{\lambda_{\mathrm qr}}{\mathrm{X}_{\mathrm lr}} \right] \tag{17}$$

where,  

$$\lambda_{mq} = X_{ml} \left[ \frac{\lambda_{qs}}{X_{ls}} + \frac{\lambda_{qr}}{X_{lr}} \right]$$

$$\lambda_{md} = X_{ml} \left[ \frac{\lambda_{qs}}{X_{ls}} + \frac{\lambda_{qr}}{X_{lr}} \right]$$

$$X_{ml} = \frac{1}{\left( \frac{1}{X_{mr}} + \frac{1}{X_{ls}} + \frac{1}{X_{lr}} \right)}$$
(18)

To obtain the currents, therefore substitute the value of flux linkages as shown in equations (19), (20), (21), and (22).

$$i_{qs} = \frac{1}{X_{ls}} (\lambda_{qs} - \lambda_{mq})$$
 (19)

$$i_{ds} = \frac{1}{X_{ls}} (\lambda_{ds} - \lambda_{md})$$
 (20)

$$i_{qr} = \frac{i_{r}}{v_{r}} \left( \lambda_{qr} - \lambda_{mq} \right) \tag{21}$$

$$i_{ds} = \frac{1}{X_{ls}} (\lambda_{ds} - \lambda_{md})$$

$$i_{qr} = \frac{1}{X_{lr}} (\lambda_{qr} - \lambda_{mq})$$

$$i_{qr} = \frac{1}{X_{lr}} (\lambda_{qr} - \lambda_{md})$$

$$(20)$$

$$i_{qr} = \frac{1}{X_{lr}} (\lambda_{qr} - \lambda_{md})$$

$$(22)$$

Based on the above equations, the torque and rotor speed can be determined as equations (25) and (26). Ferreira, et al. (2008).

$$T_{e} = \frac{3}{2} \left( \frac{p}{2} \right) \left( \lambda_{qr} i_{dr} - \lambda_{dr} i_{qr} \right)$$
 (25)

$$\omega_{e} = \int \frac{P}{2I} (T_{e} - T_{L}) \tag{26}$$

## **Methods Of Calculating Magnetsing Reactance**

The magnetizing reactance (Xm) of an induction motor can be calculated using various methods. Here are some common methods

i. Using Magnetizing Inductance Park, et al (2024).

$$Xm = \omega * Lm$$
 (27)

where: Xm = magnetizing reactance,  $\omega$  = angular frequency (2 \*  $\pi$  \* f), Lm = magnetizing inductance

ii. Using Motor Parameters

$$Xm = (V1 / Im) * sin(\theta m)$$
 (28)

where: V1 = stator voltage, Im = magnetizing current,  $\theta$ m = magnetizing current angle

iii. Using Equivalent Circuit Parameters

$$Xm = X1m * (1 + (R2 / X2))$$
 (29)

where: X1m = stator magnetizing reactance, R2 = rotor resistance, X2 = rotor reactance

iv. Using Design Data

$$Xm = (4 * \pi * f * N^2 * A) / (g * 1)$$
 (30)

where: f = f frequency, N = f number of turns, A = f cross-sectional area of the magnetic circuit, g = f air gap length 1 = length of the magnetic circuit

v. Using No-Load Test Data

$$Xm = V1 / (I0 * sin(\theta 0))$$
 (31)

where: V1 = stator voltage, I0 = no-load current,  $\theta$ 0 = no-load current angle

These equations illustrate the different methods for calculating Xm, which is an important parameter in induction motor design and analysis. The choice of method depends on the available data and the specific application.

## IV. Experimental Setup

Ammeters, voltmeters, and wattmeters were attached to measure the current, voltage, and power from the 1.5KW three-phase induction motor, which was powered by a three-phase variable voltage source. For the no-load test, the motor was let to operate.

Table 1.0: Specifications of the studied motor

	Table 1.0. Specifications of the studied motor				
Part	Parameter	Value			
Rated parameters	Rated voltage	380 V			
•	Rated current	3.80 A			
	Rated speed	1500 rpm			
	Power output	1.5 kW			
	slot numbers	34			
Stator	Outer diameter	120 mm			
	Inner diameter	75 mm			
	Pole embrace	0.45			
	Yoke thickness	12 mm			
	Frame	Mec100			
	Pole number	4			
	Rotor bar	28			
Rotor	Pole embrace	0.3			
	Yoke thickness	9 mm			
	Inner diameter	30mm			

Table 1.0 shows the rated motor specifications; these values were used in design of the motor in motor experiments and simulations were done and results gotten.

Table 2.0: Results From No Load Test

Voltage(V)	Current (Ia)	Current (Ib)	Current (Ic)	Average current	Input Power (P)	Speed (N) RPM
50	0.58	0.61	0.56	0.58	38.6	1452
70	0.49	0.55	0.42	0.48	44.8	1513
90	0.43	0.48	0.46	0.45	54.0	1525
110	0.43	0.61	0.49	0.51	74.9	1480
130	0.48	0.75	0.59	0.60	104.0	1488
150	0.60	0.71	0.71	0.67	134.0	1491
170	0.73	0.79	0.79	0.74	167.7	1493
190	0.79	0.90	0.90	0.86	217.9	1494
210	0.93	0.95	0.95	0.94	263,2	1505
230	0.97	1.06	1.06	1.03	315.9	1465
250	0.95	1.27	1.27	1.16	386.7	1464
270	1.11	1.40	1.40	1.39	500.5	1497
290	1.21	1.59	1.59	1.46	561.8	1497
310	1.24	1.84	1.84	1.64	678.0	1498
330	1.40	1.77	1.77	1.65	726.2	1498
350	1.54	1.97	1.97	1.82	849.5	1498
370	1.58	2.05	2.05	1.89	932.6	1498
380	1.72	2.18	2.18	2.02	1027	1498
390	2.02	2.24	2.24			1498

# V. Result Presentation And Discussion Rm=0.5

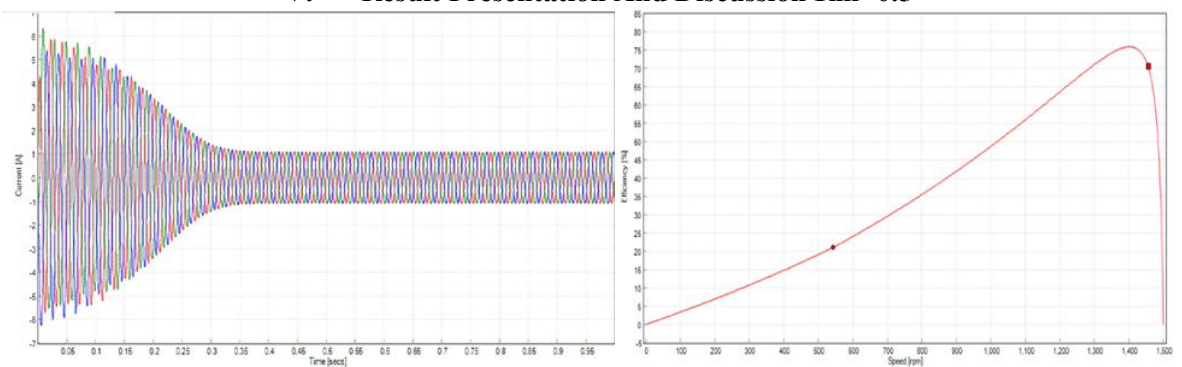


Fig. 1.0: graph efficiency against speed at Rm=1 Fig.1.2: graph of Current against Time when Rm=1.

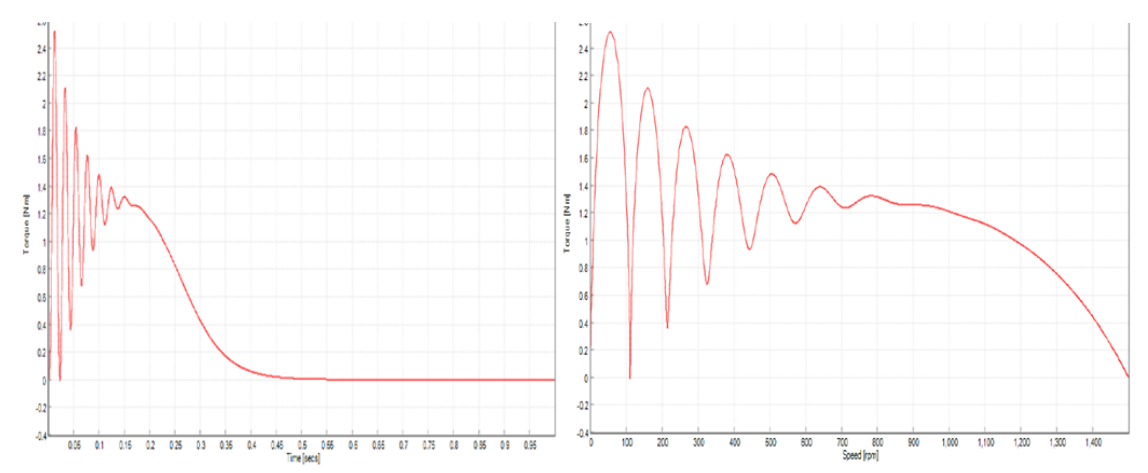


Fig. 1.3: graph of torque against time when Rm=1. Fig. 1.4: graph of torque against speed when Rm=1.

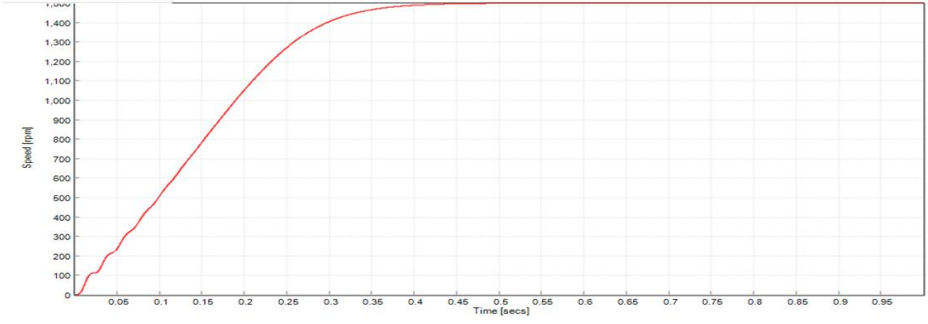


Fig. 1.5: Graph of speed against time **AT RM = 1.5** 

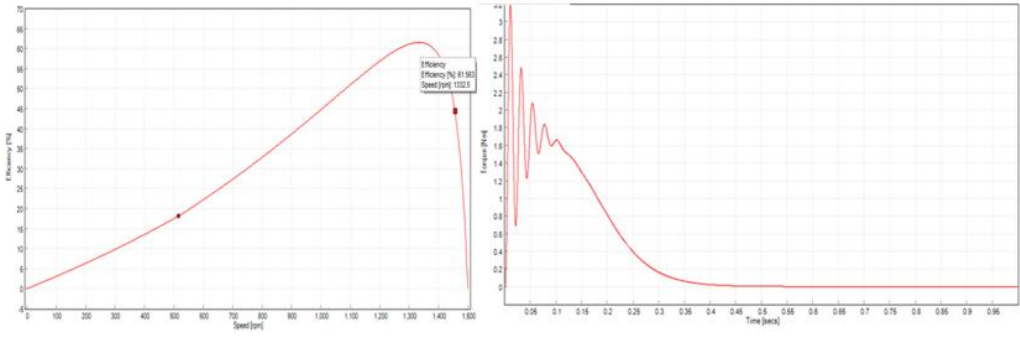


Fig. 2.0: graph efficiency against speed at Rm=0.5 Fig. 2.2: graph of torque against time when Rm=0.5.

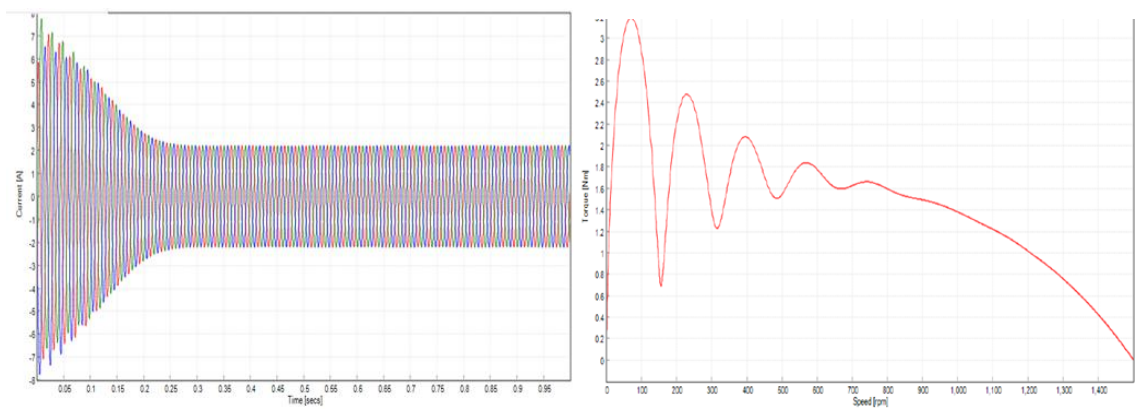


Fig. 2.3: graph of Current against Time when Rm=0.5. Fig. 2.4: graph of torque against speed when Rm=0.5.

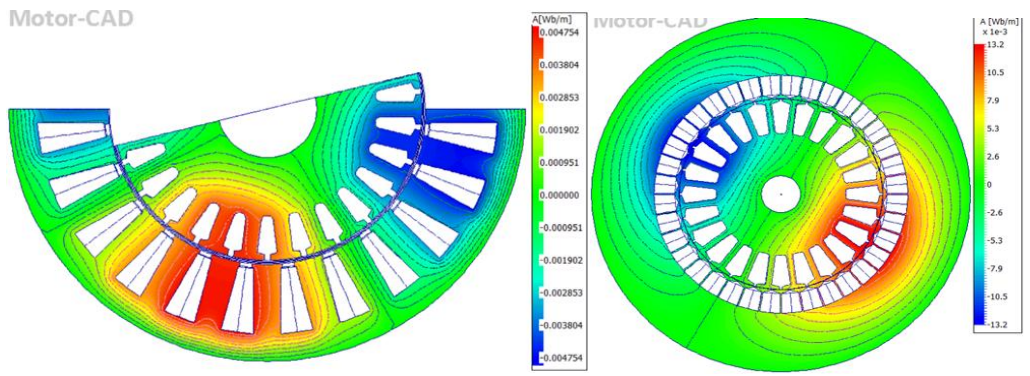


Figure 4.1: E-magnetic model showing flux distribution Fig. 4.2: E-magnetic model showing flux distribution **AT RM = 2.5** 

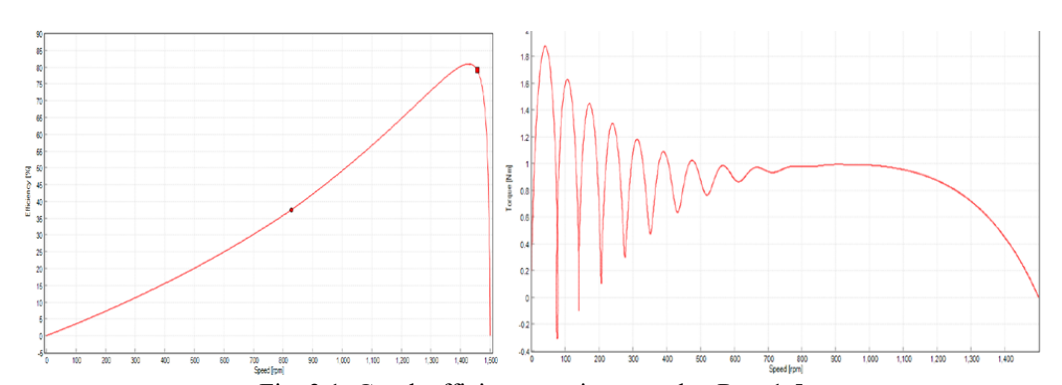


Fig. 3.1: Graph efficiency against speed at Rm=1.5 Fig. 3.2: graph of torque against speed when Rm=1.5.

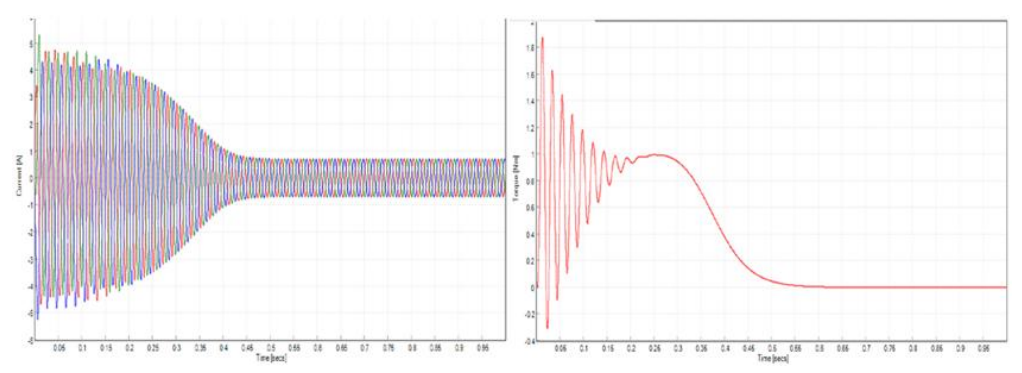


Fig. 3.3: graph of Current against Time when Rm=1.5. Fig. 3.4: graph of torque against time when Rm=1.5.

Table 2.0: motor performance result summary at the rated speed of 1500rpm from simulation

Magnetization reactance	0.5	1.0	1.5	2.5
(Rm) values				
Efficiency (%)	61.5	75	80	85
Torque (N/m)	3.2	2.55	1.82	0.3
Current (A)	3.3	1.2	1.1	1.0
Power factor (%)	75	80	70	76

## VI. Discussion Of Results

The motor rating values utilized in the studies are displayed in Table 1. This covers the parameters of the rotor and stator. Following the process, no load test was performed. Table 2.0 displays the experiment's findings. The voltage (V), current (A), power (W), and motor speed (rpm) at each voltage value are changed in this table. The rated voltage and speed are 2.22A and 1200w, respectively. After a 20-minute break, the trial findings were collected. MotorCAD software was used to further analyze the effects of changing Rm values on motor performance using the rating parameters listed in table 1.0. The effect's outcomes are displayed in Figures 1, 2, and 3. Rm can have values between 0.5, 1.0, 1.5, and 2.5. Figures 1.1, 1.2, 1.3, 1.4, and 1.5 consist of the efficiency vs speed, current versus time, torque versus speed, torque versus time, and speed versus time graphs, respectively, presented in Figure 1. Figure 1.1 shows that at a speed of 1450 rpm, the efficiency is 75%. The current in Fig. 1.2 starts at 5.6A at 0.01 seconds and stabilizes at 1.8A at 0.3 seconds. At 0.5 seconds and 75 rpm, the beginning torque in Figures 1.3 and 1.4 is 2.55 Nm. Figure 2.1 shows an efficiency of 61.56% at 1332 rpm when Rm is 0.5. Figure 2.2 shows a torque of 3.2 Nm at startup, Figure 2.3 shows a current of 7.8A at 0.01 seconds and 2.8A at 2 seconds. The efficiency in Fig. 3.1 is 80%. Rm was 1.5 when this took place. at this time, the torque is 1.82Nm, the beginning current is 5.2A, and at 4.5seconds the current is 0.8A

#### VII. Conclusion

The magnetization reactance (Xm) is critical in calculating the core and copper losses in a three-phase induction motor. Higher Xm values result in greater core and copper losses and lower efficiency, particularly during light and full load situations. Reducing Xm, on the other hand, can help enhance the motor's efficiency performance by lowering losses and increasing the power factor. On the other hand, the best value of Xm is the result of a trade-off between different elements, and motor design requires careful consideration of multiple parameters to obtain the desired efficiency and performance for specific applications. A three-phase induction motor's magnetization reactance (Xm) significantly affects its torque performance. The magnetization reactance is a part of the rotor's equivalent circuit and represents the reactance associated with the magnetizing current required to establish the magnetic field in the motor's rotor. Here's how changes in the magnetization reactance (Xm) impact the torque performance of a three-phase induction motor are as follows; During motor starting, a significant amount of torque is required to overcome inertia and accelerate the load. The starting torque is directly related to the magnetizing current and the magnetization reactance (Xm). Higher Xm values lead to higher magnetizing current, resulting in a stronger magnetic field and increased starting torque. Conversely, reducing Xm can reduce the magnetizing current and, consequently, the starting torque. The pull-up torque is the maximum torque a motor can produce during starting before it slips out of synchronism. It is essential for starting loads with high inertia. A higher Xm value generally leads to higher pull-up torque, while a lower Xm reduces the pull-up torque. The breakdown torque is the maximum torque an induction motor can produce without stalling or tripping the overload protection. Changes in Xm can affect the breakdown torque, but the impact is not as straightforward as with starting torque. Other design parameters, such as rotor resistance and leakage reactance, also play significant roles in determining the breakdown torque. The magnetization reactance influences the magnetic field distribution in the motor. A higher Xm can reduce torque ripple, resulting in smoother operation and reduced mechanical vibrations. The synchronous speed of an induction motor is given by the formula: Synchronous Speed (RPM) = (120 \* Frequency) / Number of Poles. Changes in Xm can slightly affect the effective number of poles, thereby impacting the synchronous speed of the motor. The magnetization reactance affects the magnetizing current and, consequently, the overall motor performance at full load. Higher Xm values can lead to higher copper losses due to increased magnetizing current, affecting the motor's full-load torque. It's essential to optimize the magnetization reactance (Xm) along with other design parameters to achieve the desired torque performance for specific applications. A well-balanced motor design involves considering torque requirements, efficiency, starting characteristics, and other factors to ensure optimal performance under various operating conditions. Manufacturers use advanced design tools and simulations to achieve a given application's most suitable magnetization reactance and overall motor performance

#### References

- [1]. Okoro, I. O. Computer Simulation Of A Squirrel-Cage Induction Machine With Non-Linear Effects.
- [2]. Okoro, O. I. (2003) Steady State And Transient Analysis Of Induction Motor Driving A Pump Load. Nigerian Journal Of Technology, 22(1), 46-53.2003

- [3]. Eke, A., Fischer, G., David, A., Ekpenyong, O., & E.J, Akpama. (2024) The Effect Of Rotor And Stator Slot Numbers On The Performance Of Three-Phase Induction Motors Used For Transport Application. 2024
- [4]. Perduková, D., Palacký, P., Fedor, P., Bober, P., & Fedák, V. Dynamic Identification Of Rotor Magnetic Flux, Torque And Rotor Resistance Of Induction Motor. IEEE Access, 8, 142003-142015. 2020.
- [5]. Yilmaz, M. (2015) Limitations/Capabilities Of Electric Machine Technologies And Modeling Approaches For Electric Motor Design And Analysis In Plug-In Electric Vehicle Applications. Renewable And Sustainable Energy Reviews, 52, 80-99.
- [6] Ejiofor, S. O., Abuchi, N. C., Damian, N., & Okoro, O. I. (2015) Performance Study Of Three-Phase Induction Motor Driving A Load. Discovery Journals, 55(282), 279-290.
- [7]. Matsushita, M., Ishibashi, F., & Mizuno, S. (2016) Calculation Of Magnetizing Inductance And Magnetizing Current Of Squirrel Cage Induction Motor.19th International Conference On Electrical Machines And Systems (ICEMS), 1-5.
- [8]. Park, S. H., Chin, J. W., Cha, K. S., Ryu, J. Y., & Lim, M. S. (2023) Investigation Of AC Copper Loss Considering Effect Of Field And Armature Excitation On IPMSM With Hairpin Winding. IEEE Transactions On Industrial Electronics, 70(12), 12102-12112.
- [9]. Ghosh, S., Gupta, A., Dashora, H., & Ranjan, S. (2020) Mathematical Approach To Generate Efficiency Maps For Induction Motor And Optimization For EV. In 2020 IEEE First International Conference On Smart Technologies For Power, Energy And Control (STPEC) (Pp. 1-6). IEEE. September 2020
- [10] Aoyama, M., Tsuya, H., Hirata, S., & Sjöberg, L. (2021) Experience Of Toroidally Wound Double Rotor Axial-Gap Induction Machine With Soft Magnetic Composites. IEEE Open Journal Of Industry Applications, 2, 378-393. 2021
- [11]. Banchhor, D. K., & Dhabale, (2018) A. Design, Modeling, And Analysis Of Dual Rotor Axial Flux Induction Motor. In 2018 IEEE International Conference On Power Electronics, Drives And Energy Systems (PEDES) (Pp. 1-6). IEEE. December 2018.
- [12]. Ejiofor, S. O., Abuchi, N. C., Damian, N., & Okoro, O. I. (2019). Performance Study Of Three-Phase Induction Motor Driving A Load. Discovery, 55(282), 279-290.
- [13]. Dey, A., Tripathi, A., Singh, B., Dwivedi, B., & Chandra, D. (2008). An Improved Model Of A Three-Phase Induction Motor Incorporating The Parameter Variations. Electrical Power Quality And Utilisation. Journal, 14(1), 73-78.
- [14]. Sengamalai, U., Anbazhagan, G., Thamizh Thentral, T. M., Vishnuram, P., Khurshaid, T., & Kamel, S. (2022). Three Phase Induction Motor Drive: A Systematic Review On Dynamic Modeling, Parameter Estimation, And Control Schemes. Energies, 15(21), 8260.
- [15]. Ali, A. J., Shanshal, A. K., Aziz, H. E., & Hussain, E. (2024). Characteristic Optimization Of Three-Phase Induction Motors Based On FEM.
- [16]. Montaser, M., Ibrahim Selem, S., & Enany, M. (2025). Steady State Modeling And Performance Improvement Of Induction Motor Using Different Strategy. The Egyptian International Journal Of Engineering Sciences And Technology, 51(3), 80-87.
- [17]. Ferreira, F. J., & Cistelecan, M. V. (2008, September). Simulating Multi-Connection, Three-Phase, Squirrel-Cage, Induction Motors By Means Of Changing The Per-Phase Equivalent Circuit Parameters. In 2008 18th International Conference On Electrical Machines (Pp. 1-8). IEEE.
- [18]. Ai, C., Lee, C. H., Kirtley, J. L., Huang, Y., Wang, H., & Zhang, Z. (2019). A Hybrid Methodology For Analyzing The Performance Of Induction Motors With Efficiency Improvement By Specific Commercial Measures. Energies, 12(23), 4497.
- [19]. Xu, S., & Ren, H. (2018). Analytical Computation For AC Resistance And Reactance Of Electric Machine Windings In Ferromagnetic Slots. IEEE Transactions On Energy Conversion, 33(4), 1855-1864.
- [20]. Popov, I. P. (2021). Methods For Determining The Scattering Reactance Of Transformer Windings. Russian Electrical Engineering, 92(1), 43-46.
- [21]. Liang, Y., Gao, L., Li, C., & Hu, Y. (2017). Investigation Of End Leakage Reactance And Its Influence On The Accuracy In Performance Calculation Of Large Double Canned Induction Motors. IEEE Transactions On Industrial Electronics, 65(2), 1420-1428
- [22]. Park, D. H., Song, C. H., Won, Y. J., Park, J. C., Kim, H. S., Park, H. R., ... & Lim, M. S. (2024). Magnetizing Inductance Estimation Method Of Induction Motor For Ev Traction Considering Magnetic Saturation Changes According To Current And Slip Frequency. IEEE Transactions On Magnetics.
- [23]. Park, D. H., Song, C. H., Won, Y. J., Park, J. C., Kim, H. S., Park, H. R., ... & Lim, M. S. (2024). Magnetizing Inductance Estimation Method Of Induction Motor For Ev Traction Considering Magnetic Saturation Changes According To Current And Slip Frequency. IEEE Transactions On Magnetics.